Structural, electronic, and magnetic properties of MB_n (M=Cr,Mn,Fe,Co,Ni, $n \leqslant 7$) clusters

Xia Liu,[1] Gao-feng Zhao,[1,*] Ling-ju Guo,[1] Qun Jing,[1] and You-hua Luo[1,2]
[1]*Institute of Theoretical Physics, School of Physics and Electronics, Henan University, Kaifeng 475004, China*
[2]*Department of Physics, East China University of Science and Technology, Shanghai 200237, China*
(Received 14 April 2007; published 6 June 2007)

We have investigated the stability, electronic, and magnetic properties of transition-metal-doped MB_n clusters (M=Cr,Mn,Fe,Co,Ni, $n \leqslant 7$) using first-principles density functional theory with generalized gradient approximation. The equilibrium structures of MB_n ($n \leqslant 5$) clusters can be obtained by directly adding M atoms to the B_n clusters, while for n=6, hexagon or near-hexagon geometries with a boron atom at the center ring are regarded as the ground-state structures. n=7 marks the onset of three-dimensional geometries for MB_n clusters. According to the second-order energy differences, gaps between the highest occupied molecular orbital and lowest unoccupied molecular orbital and vertical ionization potentials, we can conclude that CrB_4, CrB_7, MnB_3, FeB_3, FeB_5, FeB_7, and CoB_7 possess relatively higher stabilities. The relative orientation between the magnetic moments of the M atom and those of its neighboring B atoms mainly exhibits an antiferromagnetic alignment for CrB_n, MnB_n, and FeB_n, while it mainly shows a ferromagnetic alignment for CoB_n and NiB_n clusters.

DOI: 10.1103/PhysRevA.75.063201 PACS number(s): 36.40.Cg

I. INTRODUCTION

During the last two decades, amorphous materials have attracted much interest due to their potential industrial applications as suitable materials [1,2]. However, their properties, which are very different from those of crystalline materials [3], lack understanding. The study of the cluster size structure of amorphous systems is a prerequisite for understanding their special physical and chemical properties.

Transition-metal- (M-) based amorphous alloys as a kind of excellent magnetism material have been paid attention to by scientists [4,5]. In the cluster size, Sun *et al.* [6] investigated the structures and magnetic properties of Fe_nB ($n \leqslant 6$) clusters using density functional theory (DFT). The variation of average moment with the atomic percentage of B atom is nonlinear in Fe_nB clusters, different from the behavior of bulk amorphous Fe-B alloys. Fang and Hu [7] calculated the magnetism of Fe_nB_2 (n=1–6). The calculated average magnetic moments were less than the relevant theory calculation results of Fe_n (n=1–6) clusters and the experimental value of pure metal Fe, and totally appeared soft magnetism. Yang *et al.* [8] calculated the magnetic properties of FeB_n (n=1–6) clusters. The magnetic moment of Fe atoms and the total magnetic moment decrease with an increase of cluster size except for FeB_5. Deshpande *et al.* [9] studied the magnetic properties of Ni_nB (n=1–8,12) clusters. They pointed out that doping of boron enhances the binding energy but reduces the magnetic moments of Ni clusters. Torres *et al.* [10] investigated the element- and size-dependent electron stability of Au_nM^+ clusters (M=Sc,Ti,V,Cr,Mn,Fe,Au, $n \leqslant 9$); the environment and doping play an important role on the stability and magnetic properties of clusters. Sun *et al.* [11] studied the effect of boron impurities on the bonding in ordered intermetallic Ni_3Al using the full-potential linear-muffin-tin-orbital method. They found that changes in the electronic structure induced by boron result from the hybridization of the d state of the nearest-neighbor Ni atoms with the B p states. In our previous work, Luo and co-workers also calculated the magnetic properties of NiB_n [12] and $CoBe_n$ [13] clusters. They pointed out that the total magnetic moment of clusters oscillates with increasing size. However, in all cases, the local magnetism is very sensitive to its local structure and environment.

Stimulated by these previous investigations, in this paper we present spin-density functional calculations for a wider range of 3d dopant atom and cluster sizes—that is, MB_n (M=Cr,Mn,Fe,Co,Ni, $n \leqslant 7$) clusters. Such calculations could offer a unique opportunity to study how magnetic properties change as the local electrons of an isolated atom start to delocalized in the cluster and how the magnetism of the MB_n clusters develop with increasing cluster size.

In the following section (Sec. II), we describe in brief the computational details. In Sec. III, we present the lowest-energy structures of MB_n (M=Cr,Mn,Fe,Co,Ni) clusters and discuss their growth behavior. The electronic and magnetic properties of these clusters are also discussed. Finally, the conclusions are given in Sec. IV.

II. COMPUTATIONAL DETAILS

All calculations are based on spin-polarized DFT in the DMOL 3 package [14]. In the electronic structure calculations, an all-electron treatment and double-numerical basis including d-polarization function (DND) [14] were chosen. The exchange-correlation interaction was treated within the generalized gradient approximation (GGA) using the Perdew-Wang 1991 (PW91) [15] functional. Self-consistent field calculations were done with a convergence criterion of 10^{-6} hartee on the total energy. The density mixing criteria for charge and spin were 0.02 and 0.05, respectively. In the geometry optimization, the converge thresholds were set to 0.002 hartree/Å for the forces, 0.005 Å for the displace-

*Electronic address: zgf@henu.edu.cn

ment, and 10^{-5} hartree for the energy change.

In order to test the quality of the scheme for the description of MB_n clusters, we have first considered FeB and NiB for which theoretical data are available for comparison. For FeB, the calculated binding energy of 1.846 eV, bond length of 1.744 Å, and multiplicity of 4 are all consistent with previous DFT results of 2.15 eV, 1.78 Å, and 4 by Sun *et al.* [6], while for NiB, the calculated binding energy of 2.024 eV, bond length of 1.705 Å, and multiplicity of 2 are all consistent with previous DFT results of 2.46 eV, 1.46 Å, and 2 by Deshpande *et al.* [9]. We also calculated the B_2 dimer and the triplet B_2 is the most stable structure; the B-B bond length, vibrational frequency, and binding energy per atom are 1.604 Å, 937.85 cm^{-1}, and 1.547 eV, respectively. This result is in good agreement with the experimental values of 1.59 Å, 1051.3 cm^{-1}, and 1.54 eV [16]. Therefore, we have confidence to use the same basis set throughout the whole calculation.

For each initial structure, previous studies of the boron, chromium, manganese, iron, cobalt, and nickel clusters are seen as a guide, and all possible MB_n clusters are considered. The stabilities of MB_n were examined by evaluating the harmonic frequencies. For each of these clusters, all computed frequencies were confirmed as real. In this paper, spin-unrestricted calculations were performed for all allowable spin multiplicities. We started with a spin-singlet configuration for the even-electron systems and a spin-doublet configuration for the odd-electron systems until the energy minimum was reached. For each stable structure, binding energies per atom (E_b), vertical ionization potentials (VIPs), and energy gaps (E_g) of MB_n clusters were calculated and discussed. The on-site charges and magnetic moment were evaluated via Mulliken population analysis.

III. RESULTS AND DISCUSSIONS

A. Equilibrium geometries

The lowest-energy structures of MB_n (M=Cr,Mn,Fe,Co,Ni, $n \leqslant 7$) clusters are shown in Fig. 1. The structures of B_n clusters are also presented for comparison. The grounds states of B_n clusters examined are all singlet with even n while those of the clusters with odd n are all doublet. The equilibrium structures of B_n clusters (n=2–8) are all planar geometries which can be obtained by adding one boron atom to one side of the B_{n-1} structures, performing a zigzag-ladder-like structure. This result is in good agreement with previous theoretical work [17].

For MB_n ($n \leqslant 7$) clusters, according to our calculations, the ground states (spin multiplicity) of MB_n (M=Cr,Mn,Fe,Co,Ni, $n \leqslant 7$) clusters follow the sequence 6,3,4,5,6,3,4; 5,4,5,4,3,2,3; 4,3,4,3,2,3,2; 3,2,3,2,3,2,1; and 2,1,2,1,2,1,2. As a general trend, we obtain planar geometries for the lowest-energy isomers of MB_n clusters with $n \leqslant 6$ and three-dimensional (3D) geometries for MB_n clusters with n=7. The exceptions are CoB_6 and NiB_6, which are 3D. To confirm that the structures obtained by our calculations are the ground state, we also carried out geometry optimizations at the DFT/B3LYP/6-311+G (d) level for the MB_n ($4 \leqslant n \leqslant 6$) clusters, and calculations using the GAUSSIAN 03 package [18] further confirm that MB_n ($n \leqslant 6$) clusters are favorable for forming planar structures (B3LYP denotes the Becke three-parameter Lee-Yang-Parr hybrid functional).

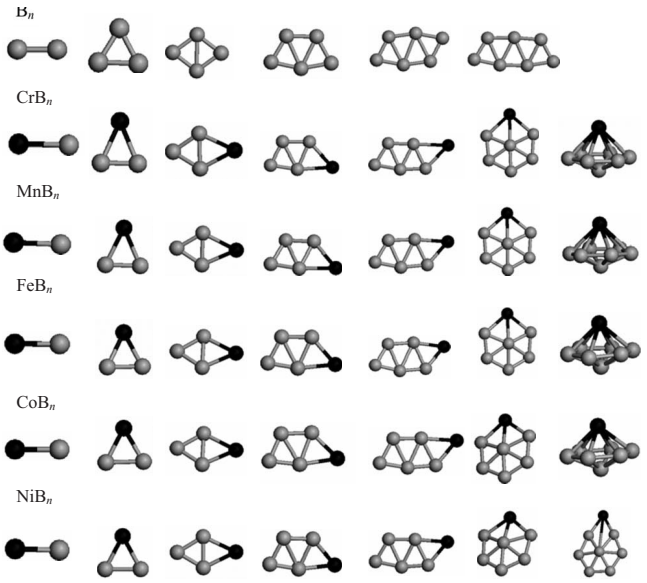

FIG. 1. Equilibrium geometries of MB_n (M=Cr, Mn, Fe, Co, Ni, B, $n \leqslant 7$) clusters.

From another perspective, the ground-state structures of MB_n ($n \leqslant 5$) clusters can be obtained by directly adding M atoms to B_n clusters, resembling the B_{n+1} species, while for n=6, hexagon (CrB_6, MnB_6, and FeB_6) or near-hexagon (CoB_6 and NiB_6) geometries with a boron atom at the center ring are regarded as the ground-state structures. In fact, we also find 2D isomers of MB_6 clusters resembling the B_7 species, but they are higher in energy than the equilibrium structures. It may be mentioned at this point that several planar geometries were optimized to verify the preference of CoB_6 and NiB_6 to follow the trend of the planar structure motif and a few of the planar structures ultimately converged to a nonplanar structure. As one goes to MB_7, hexagonal bipyramids with M atoms at the apical site were obtained as the lowest-energy structure except for NiB_7 which is a side-adsorbed hexagonal pyramid. In a sense, we can say that n=7 marks the onset of 3D geometries for MB_n clusters. This result is in good agreement with previous DFT calculations for Au_nM^+ (M=Sc,Ti,V,Cr,Mn,Fe,Au, $n \leqslant 9$) clusters which also shows that the 3D geometries begin at n=7 by Torres *et al.* [10]. As Au_n and B_n all hold planar geometries for small cluster size and have an electronic configuration of (Au) $4d^{10}5s^1$ and (B) $2s^22p^1$, respectively, there may be similarity in geometry between the Au_nM and MB_n clusters, and such consistency further confirms the reliability of our calculations.

B. Electronic and magnetic properties

We now discuss the size-dependent physical properties of these clusters. The binding energy per atom (E_b), highest

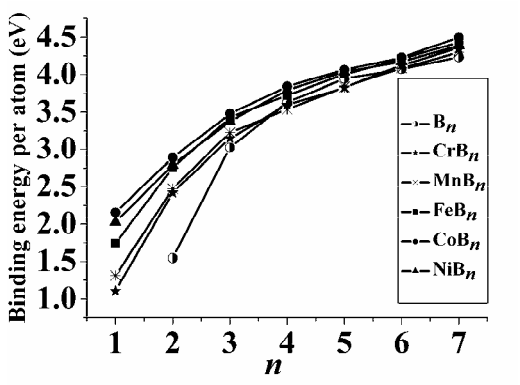

FIG. 2. Binding energies per atom E_b (eV) for the most stable isomers of MB_n (M=Cr, Mn, Fe, Co, Ni, $n \leqslant 7$) and B_n ($n \leqslant 7$) clusters.

occupied and lowest unoccupied molecular orbital (HOMO-LUMO) gaps (E_g), and VIPs of MB_n clusters are shown in Fig. 2, Fig. 3, and Table I. As seen from Fig. 2, all curves show that the binding energies generally increase with cluster size. Thus the clusters can continue to gain energy during the growth process. The binding energies of MB_n ($n \geqslant 2$) clusters are larger than those of pure B_n except for CrB_4, MnB_4, CrB_5, and MnB_5. So the doping of M atom improves the stability of B_n clusters.

In cluster physics, the second-order difference of cluster energies, $\Delta_2E(n)=E(n+1)+E(n-1)-2E(n)$, is a sensitive quantity that reflects the relative stability of clusters. Figure 3 shows the second-order difference of cluster total energies, $\Delta_2E(n)$, as a function of the cluster size. Maxima are found at CrB_4, CrB_7, MnB_3, FeB_3, FeB_5, FeB_7, CoB_7, and NiB_7, indicating that these clusters possess higher stability. In Fig. 3, we also present the difference between the eigenvalues of the LUMO and HOMO, known as the HOMO-LUMO gap. In addition, the VIP is another factor that reflects cluster stability; such data are also presented in Fig. 3. It is currently believed that large gaps and high VIPs are good indicators of the stability of clusters. As seen from Fig. 3, all these factors show that CrB_4, CrB_7, MnB_3, FeB_3, FeB_5, FeB_7, and CoB_7 possess higher stability than their neighbor's sizes, while for NiB_n ($n \leqslant 7$), no magic number was found in the range of $n \leqslant 7$ by our calculation, and this result is in agreement with our group's previous calculation [12]. So it will be necessary to extend the present study into the region of NiB_n clusters of intermediate size, with $8 \leqslant n \leqslant 20$.

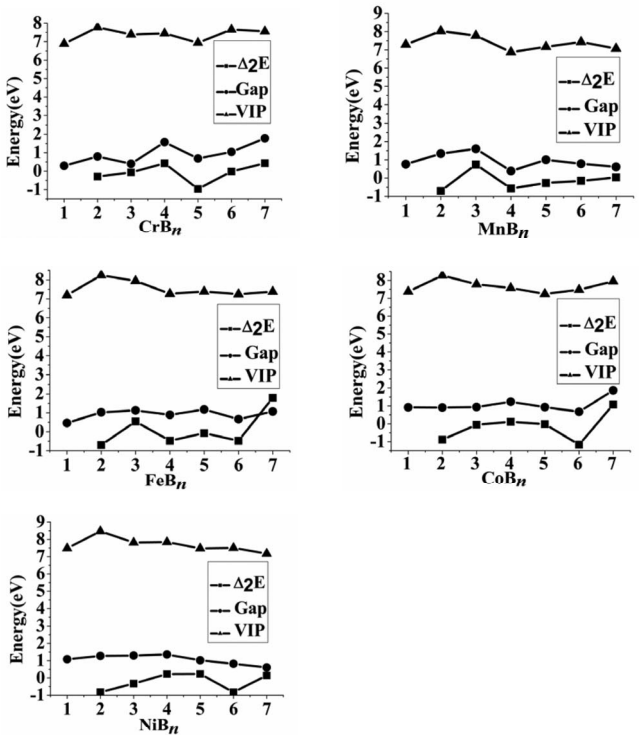

FIG. 3. The second-order energy difference, HOMO-LUMO gaps (eV), and the vertical ionization potentials (eV) of MB_n (M=Cr, Mn, Fe, Co, Ni, $n \leqslant 7$) clusters.

We perform Mulliken population analysis for the lowest-energy structures, and the atomic charges of the M atom of the MB_n clusters are listed in Table I. For MB_n clusters, charge transfers from M atom to B atoms. As seen from Table I, maxima are found at MnB_3, CrB_3, CrB_7, FeB_3, FeB_7, CoB_3, CoB_7, NiB_3, and NiB_6, which are consistent with the result shown in Fig. 3 except for NiB_3 and NiB_6. Thus, to such an extent, we can say that the mechanism of charge transfer between atoms influences the stability of the clusters. The larger the charge transfer, which results in a stronger hybridization with the host, the higher the cluster stability. Table I also shows that the charge of the Cr atom is well below $0.40e$ except for CrB_7 ($0.419e$) and there is a weak charge transfer [around $(0.02-0.2)e$, except for MnB_7 and FeB_7] from the M atoms to B atoms for MB_n (M=Mn,Fe,Co,Ni) clusters. For the small cluster size, the M-B bond is mainly covalent, and the amount of charge transfer to B atoms follows roughly the sequence of the electronegativity difference between B and M atoms.

Based on the optimized geometries, the magnetic properties of MB_n clusters were investigated and the results are presented in Table I. For CrB_n and MnB_n ($n \leqslant 7$) clusters, the total magnetic moment [about $(2-5)\mu_B$, $(1-4)\mu_B$] is mainly located on the Cr or Mn atom; most of the local moments on B atoms were found to align antiferromagnetically with respect to that on the Cr or Mn atom expect for CrB, CrB_5, and MnB_3, which show a ferromagnetic alignment. For FeB_n ($n \leqslant 7$) clusters, the total magnetic moment is about $(1.1-3.0)\mu_B$ and is mainly located on the Fe atom. A small amount of spin [about $(0.1-0.4)\mu_B$] was found on the B sites, while most of the local moments on B atoms were found to align antiferromagnetically with respect to that on Fe atom except for FeB_3. However, the magnetic moment on Fe atom is smaller than the bulk moment ($2.21\mu_B$) except for that of the FeB_3 and FeB_4 which are little larger ($0.384\mu_B$ and $0.104\mu_B$, respectively) than the bulk moment.

The total magnetic moment of CoB_n ($n \leqslant 6$) as a function of the cluster size shows pronounced odd-even effects. The values are all $2\mu_B$ with odd n while those of the clusters with even n are all $1\mu_B$. The total magnetic moment is mainly located on the Co atom [which is larger than the bulk moment ($1.17\mu_B$) except for CoB_6 and CoB_7], while most of the

TABLE I. Symmetries, binding energies per atom E_b (eV), HOMO-LUMO gaps E_g (eV), VIPs (eV) of MB_n clusters, atomic charges (e) at the M atom, magnetic moment (μ_B) of the M atom, and the total magnetic moment (μ_B) of MB_n clusters for the lowest-energy structures.

Cluster	Symm	E_b	VIP	E_g	Charge	Magnetic moment on M	Total magnetic moment
B_2	$D_{\infty h}$	1.546555		0.943568			
B_3	D_{3h}	3.023729		1.190979			
B_4	D_{2h}	3.634514		2.334195			
B_5	C_{2v}	3.946536		1.52777			
B_6	C_{2h}	4.075993		0.852448			
B_7	C_1	4.238226		0.583059			
CrB	$C_{\infty v}$	1.108306	6.890271	0.289707	0.107	4.79	5
CrB_2	C_{2v}	2.41953	7.780718	0.791248	0.216	3.412	2
CrB_3	C_{2v}	3.148527	7.392062	0.397283	0.239	3.37	3.001
CrB_4	C_s	3.5986	7.45058	1.572813	0.187	4.118	4
CrB_5	C_s	3.827947	6.942381	0.689139	0.203	4.415	4.999
CrB_6	C_s	4.129403	7.656441	1.041787	0.182	3.133	2
CrB_7	C_{6v}	4.357807	7.562963	1.778826	0.419	3.371	3
MnB	$C_{\infty v}$	1.310894	7.292976	0.756459	0.075	4.138	4
MnB_2	C_{2v}	2.471789	8.034608	1.334242	0.186	3.639	2.999
MnB_3	C_s	3.229426	7.781012	1.601672	0.228	3.929	4
MnB_4	C_s	3.536395	6.87699	0.378787	0.164	3.67	3.001
MnB_5	C_s	3.836799	7.16763	0.999192	0.147	3.17	2
MnB_6	C_s	4.089634	7.434962	0.78113	0.119	2.016	1
MnB_7	C_1	4.298999	7.076556	0.612952	0.329	2.334	1.999
FeB	$C_{\infty v}$	1.745874	7.19072	0.459952	0.106	3.259	3
FeB_2	C_{2v}	2.75118	8.24738	1.028133	0.152	2.036	2
FeB_3	C_{2v}	3.428576	7.942751	1.127685	0.202	2.594	2.999
FeB_4	C_s	3.726762	7.270264	0.89507	0.161	2.314	2
FeB_5	C_s	4.004731	7.383309	1.176699	0.134	1.832	1
FeB_6	C_s	4.21362	7.24831	0.666699	0.245	2.121	2.001
FeB_7	C_{6v}	4.429973	7.376711	1.070266	0.374	1.343	1
CoB	$C_{\infty v}$	2.154523	7.372503	0.91751	0.021	1.93	2
CoB_2	C_{2v}	2.889009	8.273965	0.907011	0.083	1.148	1
CoB_3	C_{3v}	3.479157	7.781131	0.936768	0.132	1.679	2
CoB_4	C_s	3.843271	7.574335	1.235043	0.064	1.279	1
CoB_5	C_s	4.067747	7.243945	0.933586	0.062	1.544	2
CoB_6	C_s	4.230231	7.473812	0.673254	0.029	0.751	1
CoB_7	C_1	4.498489	7.948117	1.87155	0.17	0	0
NiB	$C_{\infty v}$	2.024046	7.486631	1.085579	0.014	0.59	1
NiB_2	C_{2v}	2.789783	8.470629	1.27296	0.084	0	0
NiB_3	C_{2v}	3.377424	7.813913	1.293822	0.144	0.451	1
NiB_4	C_s	3.795772	7.841763	1.356491	0.065	0	0
NiB_5	C_s	4.037291	7.479785	1.022312	0.08	0.216	0.999
NiB_6	C_1	4.177024	7.507469	0.816435	0.179	0	0
NiB_7	C_1	4.38536	7.176747	0.605091	0.054	0.026	1

local moments on B atoms were found to align ferromagnetically with respect to those on Co atoms except for CoB_2 and CoB_4. However, the magnetic moment of Co atom is quenched at $n=7$. While for NiB_n with odd n, the total magnetic moment is $1\mu_B$, whereas for even n, the value is zero. The $1\mu_B$ moment is just required by the fact that the cluster possesses an odd number of total elements, and this result is in agreement with the results of Lei *et al.* [12]. Different from CrB_n, MnB_n, FeB_n, and CoB_n clusters, the magnetic moment located on the Ni atom is small [about

TABLE II. The charge (e) and magnetic moment (μ_B) of $3d$, $4s$, and $4p$ states for M atom in MB_n (M=Cr, Mn, Fe, Co, Ni, $n \leqslant 7$) clusters.

	$3d$		$4s$		$4p$	
Cluster	Charge	Magnetic moment	Charge	Magnetic moment	Charge	Magnetic moment
CrB	4.884	4.086	0.9	0.694	0.12	0.013
CrB_2	4.749	3.136	0.901	0.276	0.159	0.004
CrB_3	4.841	3.115	0.775	0.244	0.168	0.017
CrB_4	4.869	3.785	0.795	0.336	0.165	0.005
CrB_5	4.874	4.076	0.762	0.335	0.171	0.013
CrB_6	4.895	2.971	0.688	0.168	0.258	0.001
CrB_7	4.848	3.257	0.37	0.06	0.374	0.063
MnB	5.867	3.421	0.944	0.725	0.118	−0.003
MnB_2	5.673	3.349	0.926	0.265	0.216	0.031
MnB_3	5.737	3.642	0.821	0.256	0.209	0.038
MnB_4	5.765	3.526	0.893	0.153	0.171	−0.002
MnB_5	5.896	3.004	0.808	0.178	0.141	−0.005
MnB_6	5.983	1.85	0.665	0.176	0.228	−0.005
MnB_7	5.944	2.267	0.374	0.037	0.337	0.036
FeB	6.817	2.519	0.975	0.738	0.105	0.005
FeB_2	6.801	1.851	0.886	0.176	0.162	0.011
FeB_3	6.854	2.386	0.781	0.189	0.161	0.024
FeB_4	6.865	2.234	0.833	0.087	0.136	−0.003
FeB_5	6.977	1.744	0.768	0.094	0.117	−0.002
FeB_6	6.859	1.939	0.613	0.126	0.278	0.061
FeB_7	6.924	1.307	0.385	0.024	0.304	0.014
CoB	7.934	1.284	0.939	0.642	0.109	0.005
CoB_2	7.829	0.952	0.853	0.194	0.234	0.005
CoB_3	7.874	1.535	0.793	0.128	0.196	0.019
CoB_4	7.948	1.18	0.809	0.108	0.172	−0.006
CoB_5	7.911	1.418	0.84	0.121	0.18	0.008
CoB_6	7.938	0.686	0.705	−0.008	0.322	0.075
CoB_7	8.031	0	0.423	0	0.36	0
NiB	9.004	0.051	0.904	0.535	0.079	0.003
NiB_2	8.791	0	0.936	0	0.187	0
NiB_3	8.921	0.4	0.768	0.045	0.162	0.007
NiB_4	8.983	0	0.813	0	0.134	0
NiB_5	8.974	0.169	0.802	0.037	0.139	0.011
NiB_6	8.829	0	0.661	0	0.325	0
NiB_7	8.958	0.026	0.842	−0.003	0.139	0.003

$(0.027-0.059)\mu_B$] and is smaller than the bulk moment $(0.6\mu_B)$.

As shown by us, the relative orientation between the magnetic moments of the M atom and those of its neighboring B atoms exhibits an antiferromagnetic alignment if the M atom belongs to the early $3d$ series; it shows a ferromagnetic alignment of the M atom belongs to late $3d$ series. This result is in agreement with Andriotis and Menon's results [19]. As a result, the effective value of the magnetic moment of the M atom may appear to be enhanced or reduced. This is clearly justified in the case of CrB_n and NiB_n clusters where we find an antiferromagnetic alignment in the former and a ferromagnetic alignment in the latter; the magnetic moment for Cr atom is much larger than that of the Ni atom in NiB_n clusters.

To further understand the magnetic properties of MB_n ($n \leqslant 7$) clusters, we performed a detailed analysis of the on-site atomic charges and local magnetic moment of M atoms in MB_n clusters. The charge and spin of $3d$, $4s$, and $4p$ states for M atoms in MB_n clusters are summarized in Table II. Table II shows that the magnetic moment of M atoms is mainly from the $3d$ states, following this is the $4s$ state, and the $4p$ state contributes little to the magnetic moment of M atoms. For free Cr and B atoms, the configuration of valence electrons is $3d^5 4s^1$ and $2s^2 2p^1$, respectively. In the case of CrB_n clusters, the $4s$ and $3d$ states all lose electrons; meanwhile, the $4p$ state of Cr gains some amount of electrons. Namely, there is internal electron transfer from $4s$ and $3d$ states to the $4p$ state in Cr atoms. As mentioned above, charge transfers from Cr to B atoms. Thus, for the CrB_n clusters, the charge transfer mainly happens between Cr $4s$, $3d$, and $4p$ and B $2s$ and $2p$ states. So there exits sd-p hybridization in Cr atoms and s-p hybridization in B atoms, and there also exists strong hybridization between Cr $4s$, $3d$, and $4p$ and B $2s$ and $2p$ states.

To understand this effect, we have performed a detailed analysis of the molecular orbital by examining the electron density of the HOMO and LUMO states. As seen from Fig. 4, the d orbital of Cr exhibits a much stronger degree of hybridization with the orbitals of B, and there is strong hybridization between the s and d orbitals of Cr and the s and p orbitals of B. Thus, we may understand that there exists a mixed ionic and covalent bonding picture between Cr and B atoms, and the Cr $3d$ orbital contributes much to the Cr-B bonding.

Different from the CrB_n clusters, in the case of MnB_n, FeB_n, CoB_n, and NiB_n clusters, the $4s$ state loses electrons, and the $4p$ and $3d$ states gain some amount of electrons—that is, charge transfers from $4s$ state to $3d$ and $4p$ states of Mn, Fe, Co, and Ni—and there is strong hybridization between the $4s$ and $3d$, $4p$ states—that is, s-dp hybridization. The HOMO and LUMO of MB_n (M=Mn,Fe,Co,Ni) clusters show that the d orbital of M exhibits little degree of hybridization with the orbitals of B compared with those of in the CrB_n clusters; this may be due to the fact that the weak charge transfer from the M atom to the B atom $[(0.02-0.2)e]$ for MB_n (M=Mn,Fe,Co,Ni) clusters compared with that of the CrB_n $[(0.1-0.4)e]$ clusters.

IV. CONCLUSIONS

Using first-principles DFT-GGA calculations we have studied systematically the geometric and magnetic properties of MB_n (M=Cr, Mn, Fe, Co, Ni, $n \leqslant 7$) clusters. All the results are summarized as follows.

(i) The equilibrium structures of MB_n ($n \leqslant 5$) clusters can be obtained by directly adding the M atom to the pure B_n clusters, while for $n=6$, hexagon or near hexagon geometries with a boron atom at the center ring are regarded as the

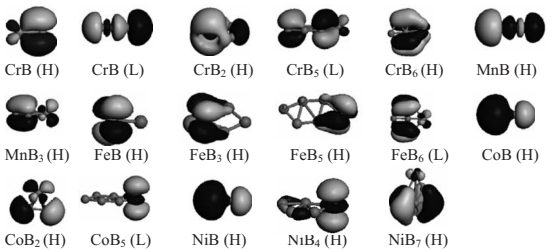

FIG. 4. The HOMO and LUMO orbitals of MB_n (M=Cr, Mn, Fe, Co, Ni, $n \leqslant 7$) clusters.

ground-state structures. $n=7$ marks the onset of 3D geometries for MB_n clusters.

(ii) From the analyses of the second-order energy difference, vertical ionization potentials, and HOMO-LUMO gaps, CrB_4, CrB_7, MnB_3, FeB_3, FeB_5, FeB_7, and CoB_7 clusters possess relatively higher stabilities, while for NiB_n ($n \leqslant 7$), no magic number was found.

(iii) Mulliken population analyses show that charge transfers from M atoms to B atoms. There is internal charge transfer from 4s and 3d states to the 4p state in Cr atoms, while for MnB_n, FeB_n, CoB_n, and NiB_n, charge transfers from 4s state to 3d and 4p states of Mn, Fe, Co, and Ni atoms.

(iv) The relative orientation between the magnetic moments of the M atom and those of its neighboring B atoms mainly exhibits an antiferromagnetic alignment for CrB_n, MnB_n, and FeB_n, while it mainly shows a ferromagnetic alignment for CoB_n and NiB_n clusters.

ACKNOWLEDGMENTS

The authors acknowledge computational support from the institute of theoretical physics of Henan University. This work is also supported by the Chinese National Science Foundation under Grant No. 10174086 and the Henan University National Science Foundation under Grant No. 06YBZR021.

[1] W. K. Klement *et al.*, Nature (London) **187**, 869 (1960).
[2] A. Böhönyey *et al.*, J. Non-Cryst. Solids **232-234**, 490 (1998).
[3] F. E. Lubrosky, *Amorphous Metallic Alloys* (Metallurgy Press, Beijing, 1989), p. 126.
[4] Y. Yamaguchi *et al.*, Adv. Cryst. Eng. **43**, 469 (2003).
[5] C. Y. Lin, H. Y. Tien, and T. S. Chin, Appl. Phys. Lett. **86**, 162501 (2005).
[6] Q. Sun, X. G. Gong, Q. Q. Zheng, and G. H. Wang, Acta Phys. Sin. **45**, 1146 (1996).
[7] Z. G. Fang and H. Z. Hu, Chin. J. Inorg. Chem. (to be published).
[8] Z. Yang, Y. L. Yan, W. J. Zhao, X. L. Lei, G. X. Ge, and Y. H. Luo, Acta Phys. Sin. (to be published).
[9] M. Deshpande, D. G. Kanhere, and R. Pandey, Phys. Rev. A **71**, 063202 (2005).
[10] M. B. Torres, E. M. Fernández, and L. C. Balbás, Phys. Rev. B **71**, 155412 (2005).
[11] S. N. Sun, N. Kioussis, S. P. Lim, A. Gonis, and W. H. Gourdin, Phys. Rev. B **52**, 14421 (1995).
[12] X. L. Lei, Y. L. Yan, W. J. Zhao, Z. Yang, and Y. H. Luo, Acta Phys. Sin. (to be published).
[13] G. X. Ge and Y. H. Luo, Acta Phys. Sin. (to be published).
[14] B. J. Delley, Chem. Phys. **92**, 508 (2000).
[15] J. P. Perdew and Y. Wang, Phys. Rev. B **45**, 13244 (1992).
[16] R. Lide David, *CRC Handbook of Chemistry and Physics*, 79th ed. (CRC Press, New York), pp. 51 and 80.
[17] A. Abdurahman, A. Skukla, and G. Seifert, Phys. Rev. B **66**, 155423 (2002).
[18] M. J. Frisch *et al.*, Computer code GAUSSIAN 03, Rev. C.02, Gaussian, Inc., Wallingford, CT, 2004.
[19] G. Mpourmpakis, G. E. Frondakis A. N. Andriotis, and M. Menon, Phys. Rev. B **68**, 125407 (2003).